AMERICAN SOCIETY FOR MICROBIOLOGY | Journal of Virology®

PATHOGENESIS AND IMMUNITY

# Reconstitution and Mutagenesis of Avian Infectious Laryngotracheitis Virus from Cosmid and Yeast Centromeric Plasmid Clones

Stephen Spatz,[a] Maricarmen García,[b] Walter Fuchs,[c] Carlos Loncoman,[d*] Jeremy Volkening,[e] Teresa Ross,[a] Sylva Riblet,[b] Taejoong Kim,[a] Nathan Likens,[a] Thomas Mettenleiter[c]

[a]US National Poultry Research Center, Athens, Georgia, USA
[b]Poultry Diagnostic and Research Center, College of Veterinary Medicine, University of Georgia, Athens, Georgia, USA
[c]Institute of Molecular Virology and Cell Biology, Friedrich Loeffler-Institut, Federal Research Institute for Animal Health, Greifswald-Insel Riems, Germany
[d]Asia-Pacific Centre for Animal Health, Melbourne Veterinary School, Faculty of Veterinary and Agricultural Sciences, University of Melbourne, Parkville, Victoria, Australia
[e]BASE$_2$BIO, Oshkosh, Wisconsin, USA

**ABSTRACT** The genomes of numerous herpesviruses have been cloned as infectious bacterial artificial chromosomes. However, attempts to clone the complete genome of infectious laryngotracheitis virus (ILTV), formally known as Gallid alphaherpesvirus-1, have been met with limited success. In this study, we report the development of a cosmid/yeast centromeric plasmid (YCp) genetic system to reconstitute ILTV. Overlapping cosmid clones were generated that encompassed 90% of the 151-Kb ILTV genome. Viable virus was produced by cotransfecting leghorn male hepatoma (LMH) cells with these cosmids and a YCp recombinant containing the missing genomic sequences - spanning the TR$_S$/UL junction. An expression cassette for green fluorescent protein (GFP) was inserted within the redundant inverted packaging site (ipac2), and the cosmid/YCp-based system was used to generate recombinant replication-competent ILTV. Viable virus was also reconstituted with a YCp clone containing a *BamH*I linker within the deleted ipac2 site, further demonstrating the nonessential nature of this site. Recombinants deleted in the ipac2 site formed plaques undistinguished from those viruses containing intact ipac2. The 3 reconstituted viruses replicated in chicken kidney cells with growth kinetics and titers similar to the USDA ILTV reference strain. Specific pathogen-free chickens inoculated with the reconstituted ILTV recombinants succumbed to levels of clinical disease similar to that observed in birds inoculated with wildtype viruses, demonstrating the reconstituted viruses were virulent.

**IMPORTANCE** Infectious laryngotracheitis virus (ILTV) is an important pathogen of chicken with morbidity of 100% and mortality rates as high as 70%. Factoring in decreased production, mortality, vaccination, and medication, a single outbreak can cost producers over a million dollars. Current attenuated and vectored vaccines lack safety and efficacy, leaving a need for better vaccines. In addition, the lack of an infectious clone has also impeded understanding viral gene function. Since infectious bacterial artificial chromosome (BAC) clones of ILTV with intact replication origins are not feasible, we reconstituted ILTV from a collection of yeast centromeric plasmids and bacterial cosmids, and identified a nonessential insertion site within a redundant packaging site. These constructs and the methodology necessary to manipulate them will facilitate the development of improved live virus vaccines by modifying genes encoding virulence factors and establishing ILTV-based viral vectors for expressing immunogens of other avian pathogens.

**KEYWORDS** *Gallid alphaherpesvirus-1*, infectious laryngotracheitis virus, origin of DNA replication, alphaherpesvirus, cosmid libraries, packaging sites, yeast centromeric plasmids

**Editor** Felicia Goodrum, The University of Arizona



Address correspondence to Stephen Spatz, Stephen.Spatz@ars.usda.gov.

*Present address: Carlos Loncoman, Instituto de Bioquimica y Microbiologia, Facultad de Ciencias, Universidad Austral de Chile, Valdivia, Chile.

The authors declare no conflict of interest.

**Received** 13 September 2022
**Accepted** 10 March 2023

Infectious laryngotracheitis (ILT), a respiratory disease of agro-economic importance to the global poultry industry (1), causes significant losses to poultry producers due to mortality, reduced weight gain, and egg production losses (2). This disease is caused by *Gallid alphaherpesvirus-1* (GaHV-1), commonly called infectious laryngotracheitis virus (ILTV), an *Iltovirus* in the subfamily of *Alphaherpesvirinae* of the family *Herpesviridae* within the order *Herpesvirales* (3). The genome of ILTV was initially characterized using Southern blot analysis, and shown to contain a type D genomic arrangement with 2 unique regions: unique long (UL) and unique short ($U_S$), with the $U_S$ sub-region flanked by inverted repeat sequences: internal repeat short ($IR_S$) and terminal repeat short ($TR_S$) (4–6). Interestingly, unlike most other alphaherpesviruses, the D-type genome of ILTV contains 3 packaging sites, pac1 and two pac2 sites (7, 8). One pac2 site is at the terminus of the UL region and links to the pac1 site at the end of the $TR_S$ region during genome circularization and concatemerization. The other site herein termed "ipac2" (for inverted pac2), is $\sim$ 800 bp downstream of the pac2 site. Its role in the life cycle of ILTV is unknown. The ILTV genome also contains 3 origins of replication: OriL within the UL region between $U_L45$ and ORFA and 2 copies of OriS within the $TR_S$ and $IR_S$ regions (4, 9). This arrangement of the replication origins is similar to those of other E-type genomes (i.e., HSV-1), except for the avian alphaherpesvirus prototype Marek's disease virus, which lacks an OriL (10).

Since the 1960s, the control of ILT has traditionally been achieved through vaccination with live attenuated strains: CEO (chicken embryo origin) (11) or TCO (tissue culture origin) (12). More recently, recombinant vaccines which use turkey herpesvirus (HVT), fowlpox virus, or Newcastle disease virus as vectors to express a limited number of envelope glycoproteins (gB, gD, and gI) have been developed for ILT control (13–17). These vaccines all protect against clinical signs; however, there are concerns about the safety of attenuated live vaccines and the efficacy of vectored vaccines (16). Although the CEO live attenuated vaccines are the most efficacious for protection against clinical disease and virus shedding, they have some shortcomings (18). A major fault is their ability to revert to virulence by simple bird-to-bird passage (19, 20). Compounding this, live ILTV vaccine strains can also establish latent lifelong infections (21).

There is a need to develop methods to design ILT vaccines rationally. Historically, attenuation of ILTV for producing the TCO and CEO vaccines was primarily an empirical process through serial passage in cultured cells or embryonated eggs. To date, 20 genes have been successfully deleted from the ILTV genome using laborious classical marker rescue experiments, and all are nonessential for *in vitro* viability (7). In addition, several ILTV vaccine candidates containing deletions in the nonessential envelope glycoproteins gM ($U_L10$), gC ($U_L44$), gG ($U_S4$), gJ ($U_S5$), gI ($U_S7$), and gE ($U_S8$); virus-specific enzymes dUTPase ($U_L50$) and thymidine kinase ($U_L23$), as well as *Iltovirus*-specific genes ORF C and pUL0, have been created and evaluated in animal studies (22). Still, only the ΔgG strain has been licensed for commercial use in Australia (4, 7, 23).

Moreover, the manipulation of the ILTV genome has been problematic. It lags behind other herpesviruses because of the lack of an infectious clone (i.e., bacterial artificial chromosome or cosmid library). Over the past 20 years, these genetic systems have been paramount in defining virus/host functions and vaccine/therapeutic vector development. For a review, see (24–36).

We have successfully introduced the mini-F cassette into the ILTV genome but have failed to identify *Escherichia coli* transformants containing completely intact ILTV genomes. Next-generation sequencing of these recombinants indicated that they contained deletions in the unusually long palindromic sequences comprising the origins of viral DNA replication (OriL and OriS). To our knowledge, there are no reports of infectious laryngotracheitis virus derived from cloned genomes or recombinant fragments contained within *E. coli*, *Saccharomyces cerevisiae*, or other hosts. The generation of ILTV mutants still relies on recombineering strategies, but nowadays, this is accelerated through CRISPR/Cas9 targeted double-stranded DNA breaks (37–39).

In this report, we reconstituted ILTV from a series of overlapping cosmid and yeast centromeric plasmids (YCp) clones derived from the DNA of a virulent strain of ILTV.

**TABLE 1** Characteristics of recombinant cosmid and YCp clones

| ILTV recombinant | Subgenomic region | Insert length (Kb) | Coordinates of inserts (USDA reference strain[a]) |
|---|---|---|---|
| pCIZ34 | $U_L$ | 45.005 | 1,072-46,076 |
| pCIS28 | $U_L$ | 40.968 | 41,899-82,865 |
| pCISB27 | $U_L$ | 39.899 | 68,905-105,802 |
| pCIZ52 | $U_L$-$IR_S$-$U_S$ | 40.898 | 97,660-140,266 |
| YCp-BC | $U_S$-$TR_S$-$U_L$ | 20.523 | 137,905-2,097 |
| YCp-KLO | $U_S$-$TR_S$-$U_L$ | 20.426 | 137,905-2,097 |
| YCp-ModKLO | $U_S$-$TR_S$-$U_L$ | 24.341 | 137,905-2,097 |

[a]GenBank Accession # MN518177.

Recombinant mutants lacking the inverted ipac2 sequence and another in which the ipac2 sequence was replaced with the GFP gene were also created and characterized. All recombinants were replicative competent *in vitro* and virulent *in vivo*. Applying the technology described herein will allow for manipulating nonessential and essential genes using INDEL and dicodon pair deoptimization strategies, thereby facilitating a better understanding of molecular mechanisms of ILTV pathogenicity.

## RESULTS

**Cloning ILTV DNA as cosmids and YCps.** An ILTV cosmid library was constructed using pSuper Cos with partially Sau3AI-digested genomic DNA. Random colonies were selected, and the sizes of the inserted ILTV DNA fragments were evaluated following digestion with NotI. Boundaries of the ILTV inserts in clones containing large inserts (39-45 Kb) were partially sequenced by dideoxy sequencing with vector-specific primers. Subsequently, the clones were digested with the restriction endonucleases XhoI, PvuI, and EcoRI to confirm the appropriate digestion patterns for the ILTV genomic insertions (data not shown). Four cosmids (pCIZ34, pCIS28, pCISB27, and pCIZ52) containing inserts with overlapping genomic coordinates collectively representing 89.9% of the genome were selected and further characterized by Illumina MiSeq sequencing. The genomic coordinates based on the USDA strain (JN542564) are provided in Table 1. Based on the USDA genome, 15,271 bp (1,073 and 14,198 bp at the 5′ and 3′ termini, respectively) map outside the coverage of the 4 cosmids (See Fig. 1). Because of this, a "Bridge" construct that traverses the $TR_S$/UL junction was assembled in the YCp vector, pYES1L (Thermofisher). This construct (YCp-BC) contains 5′ sequences with genomic coordinates that overlap those at the 3′ end of pCIZ52 by 2,358 bp at the $U_S$/$TR_S$ junction; it spans the entire $TR_S$ region and overlaps UL sequences at the 5′ end of pCIZ34 by 1,026 bp. In addition, 2 other bridge constructs (YCp-KLO and YCp-ModKLO) were created in which the inverted pac2 (ipac2) sequences (USDA map coordinates 830 to 932) were replaced individually with a BamHI RE site or a GFP/kanamycin cassette, respectively.

**Growth and stability of ILTV cosmids and YCp constructs.** There were no discernible growth differences among the bacteria containing cosmids pCIZ34, pCIS28, pCISB27, and pCIZ52 when propagated in Miller LB medium at 37°C and 42°C (Fig. 2). However, a slower growth rate was observed for the ModKLO YCp host relative to the cosmid constructs when propagated at 37°C. Notably, there were differences in the purity of cosmid DNA isolated from *E. coli* harboring pCIZ34 relative to the purity of other cosmids (pCIS28, pCISB27, and pCIZ52) isolated from the same *E. coli* strain when grown at 37°C (Fig. 3). When isolated from bacteria harvested during the exponential phase of growth at 37°C, a high level of chromosomal DNA was evidenced in restriction enzyme digests of pCIZ34 DNA. To improve upon this, different growth media (e.g., terrific broth, super broth, and 2X YT) were tested for *E. coli* propagation at 37°C. However, these growth media failed to improve the quality of the isolated cosmid DNA. Only when varying growth temperatures were tested did the purity of pCIZ34 dramatically improve. In addition to growth at 37°C, cultures were propagated in LB broth at the lower temperature of 30°C and the higher temperature of 42°C. The purity of the cosmid DNA was best when *E. coli* XL-1 MR containing pCIZ34 was propagated at 42°C. This purification anomaly may result from the induction of

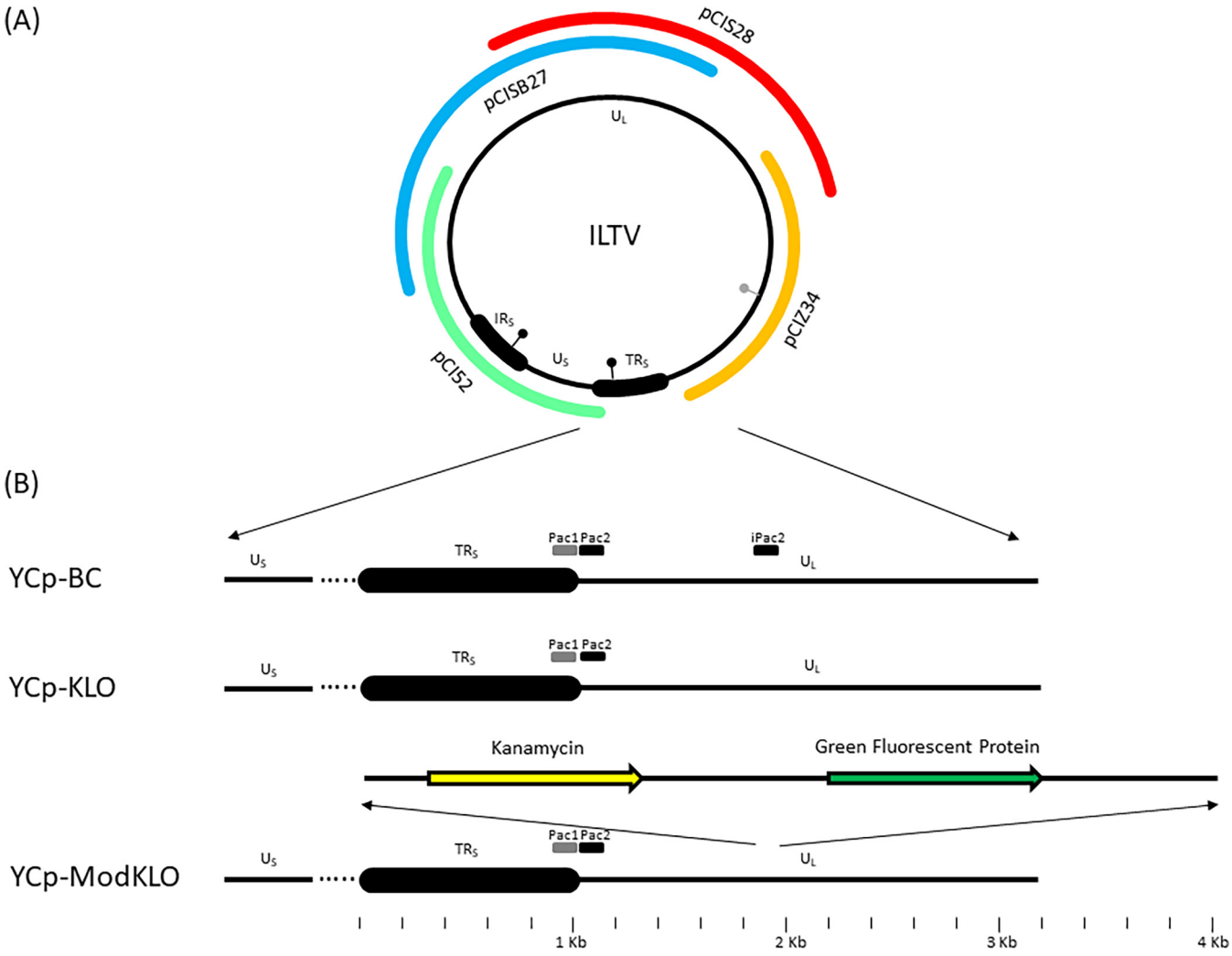


**FIG 1** The position of the overlapping cosmid and YCp inserts relative to the circular ILTV genome. (A) The 151.7 Kb ILTV genome contains 109.5 Kb unique long (UL) and a 13 Kb unique short ($U_S$) region, which are bracketed by 14.5 Kb internal and terminal inverted repeats ($IR_S$ and $TR_S$). The black lollipops represent the OriS palindromes (ΔG = -187.4 Kcal/mol) within the inverted repeats, and the gray lollipop represents the OriL palindrome (ΔG = -168.74 Kcal/mol) within the UL region. Also shown are the overlaps of the ILTV inserts within the cosmid clones (pCIZ34, pCIS28, pCISB27, and pCIZ52) and the $TR_S$/UL traversing yeast centromeric plasmids YCp-BC, YCp-KLO, and YCp-ModKLO. (B) The location of the packaging sites (pac1, pac2, and ipac2 sites) at the $TR_S$ and UL junctions of the circular ILTV genome. The yeast centromeric plasmid YCp-BC contains an insert with no alterations. The ipac2 site is deleted and replaced with a BamHI linker (YCp-KLO) or a GFP/kanamycin gene cassette (YCp-ModKLO).

heat shock proteins, which stabilized the cosmid, or a toxic gene product from a cryptic prokaryotic promoter on pCIZ34, inactivated at the higher temperature.

The stability of the exceptionally long palindromes comprising replication origins was a concern during these experiments. The 2 cosmids pCIZ34 and pCIZ52 containing OriL (268 bp) and 1 copy of OriS (280 bp), respectively, are stable within the *E. coli* XL-1 MR host, and amenable to RedET mediated recombination. We serially passaged these clones in LB broth at 37°C (pCIZ52) and 42°C (pCIZ34) for 10 days and found no deletions in the palindromes. However, once these cosmids are reintroduced into different strains of *E. coli* via electroporation, it becomes exceedingly difficult to find recombinants with intact origins of replication. To investigate this, both types of palindromes were cloned into the yeast/*E. coli* shuttle vector pYES1L via transformation-associated recombination (TAR) in yeast and screened for intactness using yeast colony PCR. Nearly 98% of the yeast recombinants contained intact OriL and OriS. Unsurprisingly, no recombinants that had intact origins could be identified after shuttling these to the common electrocompetent *E. coli* strain TOP10 (and other strains). Even when using *E. coli* strains 6262 and 6787 (ΔrecA) and 6786 (recA+) (Scarab Genomics), which were engineered to stably harbor plasmids with pronounced

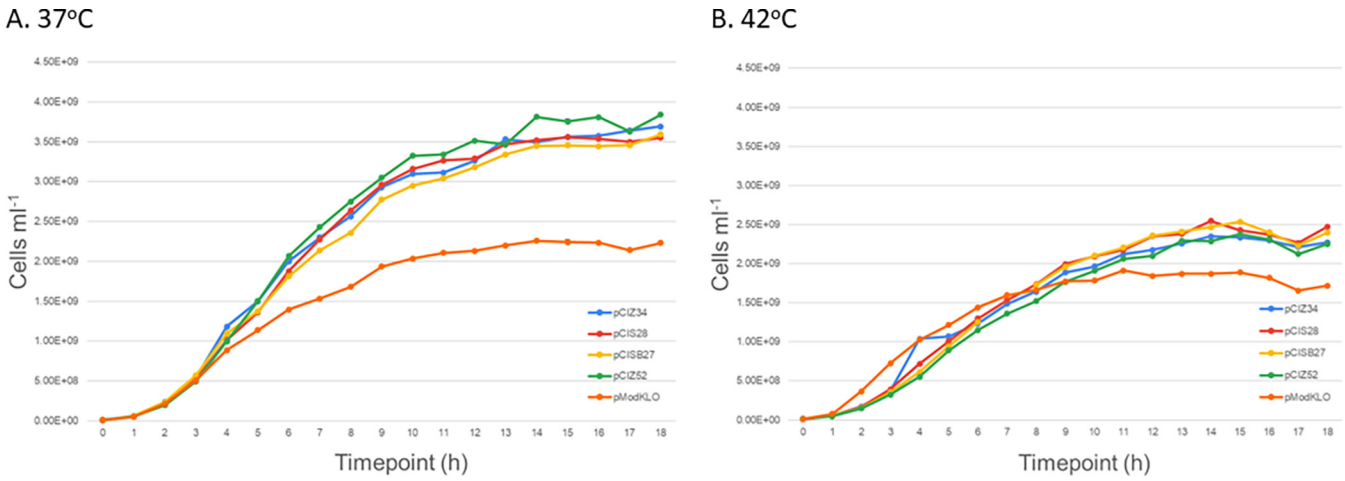


**FIG 2** Growth curves of cosmid and YCp recombinants propagated in Miller LB medium at 37°C and 42°C. Single colonies were inoculated into 5.0 mL of Miller LB broth containing 50 $\mu$g/mL of carbenicillin (for pCIZ34, pCISB27, pCIS28, or pCIZ52) or 50 $\mu$g/mL of spectinomycin (for pModKLO). After 16 h at 37°C, 100 mL of Miller LB with appropriate antibiotics were inoculated with $8.53 \times 10^6$ bacteria from the starter cultures ($t = 0$). Every hour, 1.5 mL aliquots were measured in triplicates (1:5 dilutions) at 600 nm using a Spectrophotometer 200 (Spectronic). (A) Growth at 37°C and (B) growth at 42°C.

secondary "stem-loop" structures, no recombinants were identified that contained intact origins. These strains were engineered to contain deletions in destabilizing Insertion Sequences (IS) and can harbor plasmids carrying direct repeats, inverted repeats, palindromes, or other sequences commonly unstable in standard *E. coli* strains (40). The *E. coli* recombinants had 243 nucleotides deleted in OriL and between 203 and 213 nucleotides deleted in OriS. We successfully created a YCp recombinant containing the UL insert of pCIZ34 in yeast and identified stable *E.coli* recombinants with intact origins (OriL). Similarly, YCp recombinants with inserts from pCIS28 and pCISB27 have been generated by TAR cloning in yeast and successfully transferred to *E. coli*, but we have not been able to accomplish this feat with the OriS-containing insert from pCIZ52.

**Production of infectious ILTV from cosmid and yeast centromeric plasmid clones.** Mirus transfection of LMH cells with the core set of cosmids pCIZ34, pCIS28, pCISB27, and pCIZ52 along with one of the $TR_S$/UL "bridge" clones YCp-BC, YCp-KLO, or YCp-ModKLO yielded infectious virus within 5 to 6 days (Fig. 4). Addition of recombinant vectors expressing the immediate early protein ICP4 and VP-16 (encoded by the $U_L$48 gene) to the transfection mixture enhanced infectivity (with plaques appearing earlier, sometimes by as much as 2 days earlier). While the cosmids and YCps could produce infectious virus without these ancillary plasmids, their addition increased the reliability and enhanced the efficiency of virus production. Plaque morphologies and the size of the plaques of vBC, vKLO, and vModKLO were similar to those observed with the USDA reference strain (Fig. 5). The accession numbers of the complete genome sequences of the reconstituted viruses vBC, vModKLO, and vKLO are MN784692, MN784693, and MN792995, respectively; and the USDA ILTV strain sequenced using Illumina MiSeq (USDA reference strain) is MN518177.

**Comparative sequence analysis of cosmid and YCp clones.** The pCIZ34, pCIS28, pCISB27, and pCIZ52 cosmid sequences were deposited in GenBank under the accession numbers MN784688, MN784689, MN784690, and MN784691, respectively. Sequence analysis of 77 complete ILTV genomes indicated near-perfect sequence identities of the cosmids with corresponding sequences from the genome of the USDA strain of ILTV. GenBank contains the complete nucleotide sequences of two USDA reference sequences (JN542534 and MN518177). For the cosmids pCIZ34, pCIS28, and pCISB27 with UL sequences, there was perfect sequence identity with that of the USDA (JN542534), and only 4 intragenic SNPs, which differed with the MN518177 sequence. A list of sequence differences can be found in Table 2. There were 2 different T/C substitutions in the $U_L$27 gene (gB) within pCIZ34 resulting in E189G and N678D substitutions. An A/G substitution in the $U_L$21 gene within the overlapping regions of pCIS28 and pCISB27 resulted in a synonymous substitution. A C/A substitution in the $U_S$7 gene (gI) also resulted in a synonymous substitution. Cosmid pCIZ52

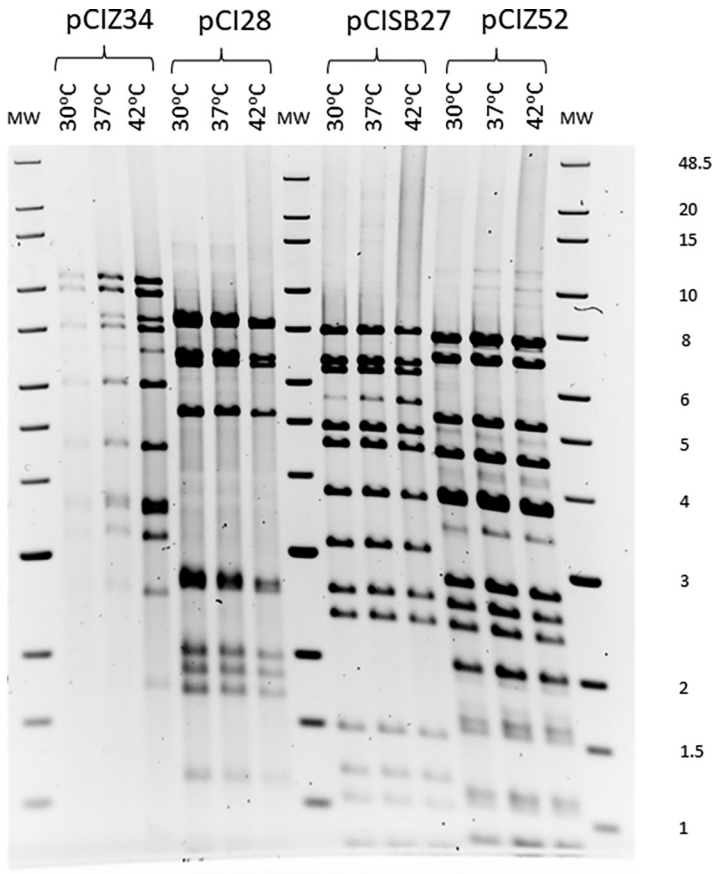


**FIG 3** Restriction digests of cosmid clones pCIZ34, pCIS28, pCISB27, and pCIZ52. *E. coli* containing the cosmids were propagated at 30°C, 37°C, and 42°C. Cells were harvested at the exponential growth phase, and DNA was purified using alkali lysis. Cosmid DNA (1.2 $\mu$g) was digested with the following restriction endonucleases: *Aat*II and EcoRV [pCIZ34]; *Asc*I and EcoRV [pCIS28]; BglII [pCISB27]; and HindIII and NheI [pCIZ52]. The DNA was separated on a 0.6% 1X TAE agarose gel for 20 h at 35 V and stained with ethidium bromide. The molecular size standards are the 1 Kb extended ladder (New England Biolabs).

contained the most genetic variations with INDELs in the 855/857 repeat region (~ 500 nuc upstream of the start codon of ICP4) and single nucleotide insertions in cytosine homopolymer stretches that flank the $U_S10$ gene.

In multiple alignments of the nucleotide sequences of the cosmids and YCps with genomic sequences of the reconstituted viruses, few base pair changes were identified. Only 2 base pair changes were identified immediately after the ipac2 site within the genomes of vModKLO and vKLO. This region is within the first 3,725 nuc of UL subgenomic region and is transcriptionally silent (unpublished results). No substitutions were identified in the vBC genome within this region.

***In vitro* growth kinetics.** The growth of recombinants vModKLO, vBC, and vKLO were measured in LMH cells (Fig. 6A). Between 0 and 24 h postinoculation, titers for USDA, vKLO, and vModKLO increased exponentially at similar rates. This contrasted with the lag growth noticed for vBC. However, by 48 h postinoculation (pi), vBC titers increased by 2 logs but never rose to the levels of USDA, vKLO, or vModKLO until 120 h pi. Statistically, there were no significant differences between the growth rates of the 4 viruses. Inspection of the entry data (Fig. 6B) might suggest a sight enhancement of entry for recombinants lacking the ipac2 sequence (vKLO with its BamHI linker and the large GFP/kanamycin cassette within vModKLO), however, this too, was not statistically significant with *P* values ranging from 0.07 to 1.0.

**Pathogenicity of reconstituted viruses after intra-tracheal/ocular administration.** The virulence of the vBC, vKLO, and vModKLO recombinants compared to the USDA parental strain in specific pathogen-free (SPF) chickens inoculated via the intra-tracheal/ocular

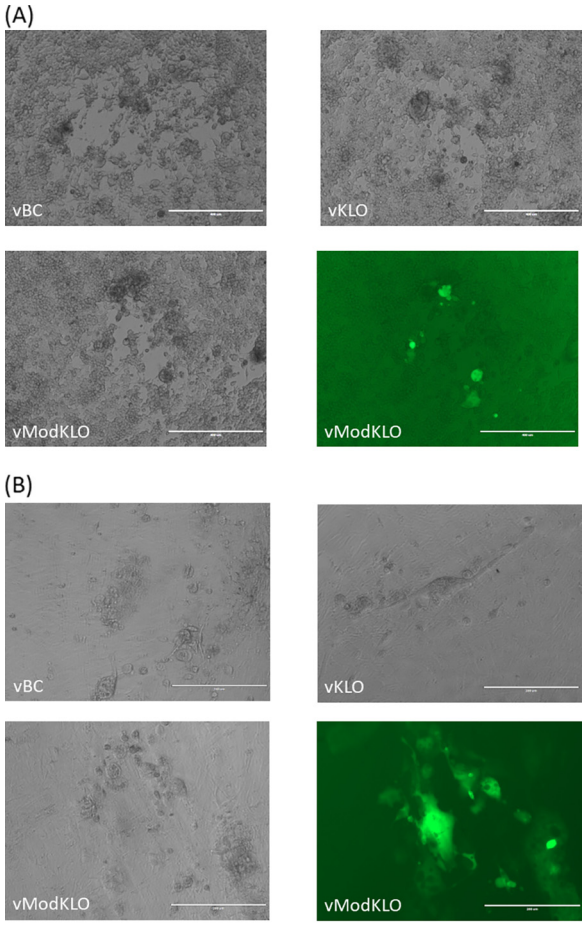


**FIG 4** Microscopic imagery of ILTV plaques in leghorn male hepatoma (LMH) and chicken kidney cells (CK). (A) LMH cells transfected with the complete set of overlapping ILTV cosmid clones (pCIZ34, pCIS28, pCISB27, and pCIZ52) and either YCp clone BC, KLO (white light images), or ModKLO expressing green fluorescent protein (GFP) (white light and green fluorescent images) at 6 days posttransfection. (B) Images of CK cells infected with the reconstituted viruses vBC and vKLO (white light images); and vModKLO expressing GFP (white light and green fluorescent images) at 3 days postinfection.

route was evaluated. At 3 days pi, the groups of chickens inoculated with the recombinant viruses and the USDA strain showed the highest clinical sign scores (CSS). Mortalities were recorded within the groups inoculated with vModKLO and the USDA parental strain (Fig. 7A). There were no significant differences ($P < 0.05$) in the median clinical sign scores of vKLO and vModKLO groups at any time point postinoculation. The median clinical sign scores observed for the vBC groups at day 4 pi were significantly lower ($P < 0.05$) than the median CSS for the USDA group, but clinical sign scores were not different at 3-, 5-, and 6-days pi (Fig. 7B). No clinical signs were observed in sham inoculated chickens. Overall, the recombinants induced significant clinical symptoms over time postinoculation. With the higher variance in the USDA group, there is no statistical support for a mean difference between the groups inoculated with the reconstituted viruses and those receiving the USDA parental control. The tracheal virus load in chickens inoculated with the recombinant viruses was not statistically different from that in chickens inoculated with the USDA strain (Fig. 8).

## DISCUSSION

Even though ILTV is an important pathogen of chickens, manipulating its genome for functional analyses of genes has been time-consuming, relying on marker rescue experiments to generate mutant viruses. CRISPR-based technologies could quicken this pace. However, the classical and gene-editing techniques are somewhat restrictive

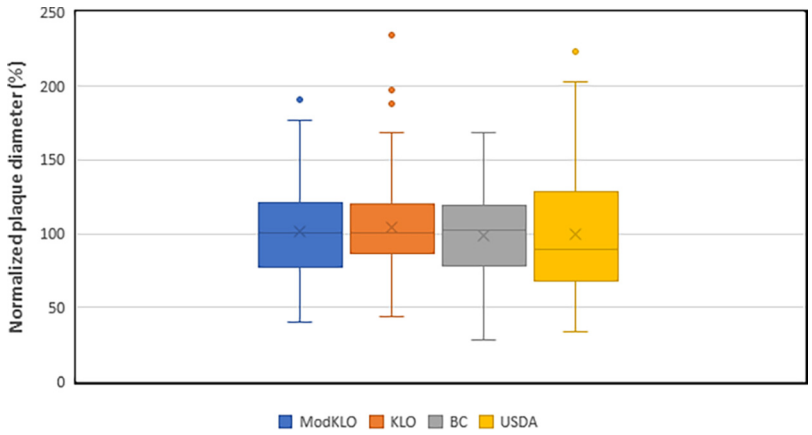


**FIG 5** Plaque sizes of the recombinant viruses. The plaques were measured at 5 dpi. Images of randomly selected plaques were captured and analyzed using the Fiji reversion of ImageJ software. The plaque size induced by the USDA reference strain was set at 100%, and mean plaque diameters are shown as box plots. Analysis was performed by one-way analysis of variance (ANOVA) with Bonferroni correction ($P > 0.05$).

since only genes dispensable for virus production are routinely manipulated. The maintenance of molecularly-defined cloned ILTV genomic fragments in *E. coli* and *S. cerevisiae* should foster the rapid and efficient mutagenesis of both essential and nonessential genes through recombineering and gene-editing strategies. However, manipulation of genes within the overlapping ends of the cosmids, which are necessary for homologous recombination, may require careful experimental design. These overlapping ends can be quite extensive (~8 to 15 kb), especially for cosmid pCISB27 and its flanking cosmids pCIS28 and pCIZ52 (Fig. 1). Alterations of both copies of the gene within these overlapping regions might be necessary before recombineering to ensure incorporation of the desired mutation in the rescued recombinant. The cosmid/YCp-based system described in this report used cloned ILTV genomic segments to reconstitute the virus without introducing undesired mutations during the recombination process. In a comparison between the nucleotide sequences of the cosmids and YCps used to reconstitute viable ModKLO and KLO viruses, only 3 single nucleotide polymorphisms were identified that differed between the input DNA (e.g., cosmids and YCps) used in cotransfection and the output viral genomic DNA (<0.002% different). None could be identified in the reconstituted BC virus.

ILTV and other alphaherpesviruses with D-type genomes (e.g., PRV, EHV-1, EHV-4, EHV-9, and SVV) contain 2 distinct packaging sites (pac1 and pac2), but, surprisingly, the ILTV genome also has an unusual packaging site, an inverted *pac*2 site (ipac2) (41). This site is located, on average, 800 bp downstream from the 5′ UL terminus/pac2 site. Interestingly, not all sequenced alphaherpesviruses with D-type genomes have this unique ipac2 site, and its function is unknown. Sequence analysis of Hirt supernatant extracts from ILTV-infected LMH cells has confirmed that the circularized genome contains the normal pac1/pac2 sites at the $TR_S$/UL junction with an ipac2 site located ~800 nuc downstream (see BC clone Fig. 1). We postulated that this redundant ipac2 site of 102 bp, which forms a large hairpin structure ($\Delta G$= -242.04 kcal/mol) with the complementing pac2, might contribute to the instability of ILTV-BACs in *E. coli* strains commonly used to maintain the genomes of other herpesviruses. The reasoning was the unusual growth properties of *E. coli* harboring cosmid pCIZ34. When propagated using standard laboratory conditions (LB broth and 37°C), pCIZ34-transformed XL1-Blue MR *E. coli* yielded low-quality cosmid DNA. After numerous trials with different media and temperatures, it was demonstrated that this clone would only yield high-quality cosmid DNA, free of chromosomal DNA contamination when propagated at 42°C (Fig. 3). This was counter-intuitive since unstable recombinant clones are usually stabilized when propagated at lower temperatures (30°C) (42). To reconstitute ILTV, cosmid pCIZ34 DNA had to be isolated from *E. coli* grown at 42°C, while *E. coli* grown at 37°C yielded

**TABLE 2** List of all differences observed between the sequences of the cosmid clones and reconstituted viruses relative to 3 USDA lineage strains (JN542534, MN518177, and KY423284) within the TCO clade[a]

| Position | Pciz34 | pCIS28 | pCISB27 | pCIZ52 | vKLO | vmodKLO | vBC | USDA MN | USDA JN | A489 | Comments |
|---|---|---|---|---|---|---|---|---|---|---|---|
| UL | | | | | | | | | | | |
| 828-833 | | | | | GGATCC | | TAATTT | TAATTT | TAATTT | TAATTT | Intragenic *BamH*I Linker in hypothetic ipac2 gene |
| 1,091 | C | | | | **A** | **A** | C | C | C | C | Intragenic hypothetic ipac2 gene |
| 1,153 | C | | | | **DEL** | **DEL** | C | C | C | C | Inttagenic hypothetic ipac2 gene |
| After 1,158 | CAC | | | | CAC | CAC | CAC | CAC | CAC | **-A-** | Intragenic hypothetic ipac2 gene |
| 18,918 | C | | | | C | C | C | C | C | **T** | Intragenic UL46 USDA/A489 Ser 203 Leu |
| 20,421 | C | | | | C | C | C | C | C | **T** | Intragenic UL45 USDA/A489 Ser 203 Leu |
| 36,135 | C | | | | C | C | C | **T** | C | C | Intragenic UL27 (gB) USDA/A489 Ser 203 Leu |
| 37,601 | C | | | | C | C | C | **T** | **T** | **T** | Intrangenic in UL27 (gB) USDA/BC Glu 189 Gly |
| 65,986 | | C | C | | C | C | C | C | C | **T** | Intragenic UL39 USDA/A489 Leu 275 Phe |
| 74,579 | | G | G | | G | G | G | **A** | G | G | Intragenic synonymous substitution in UL21 |
| 95,003 | | | T | | T | T | T | T | T | **A** | Intragenic UL8 USDA/A489 Ser 26 Thr |
| 98,127 | | | A | A | A | A | A | A | A | - | UL7 frameshift after Phe 103; 358 aa vs 120 aa |
| After 110,165 | | | | G | G | G | G | G | G | - | Intergenic poly G stretch |
| IRS | | | | | | | | | | | |
| After 112,420 | | | | C | C | C | C | C | C | - | ICP4 frameshift after Gly 1332; 1486 aa vs 1334 aa |
| 118,074 | | | | A | A | A | A | A | A | **G** | Intergenic 855/857 region |
| 118,090 | | | | A | A | A | A | A | A | **G** | Intergenic 855/857 region |
| 118,128 | | | | A | A | A | A | A | T | **A** | Intergenic 855/857 region |
| After 118,139 | | | | GT | GT | GT | GT | GT | GT | – | Intergenic 855/857 region |
| 118,159 | | | | G | **A** | **A** | G | G | G | **A** | Intergenic 855/857 region |
| 119,786 | | | | **G** | A | A | A | A | - | - | Intergenic 855/857 region |
| 119,802 | | | | **G** | A | A | A | A | - | - | Intergenic 855/857 region |
| 119,871 | | | | **A** | G | G | **A** | G | - | - | Intergenic 855/857 region |
| 120,643 | | | | C | C | C | C | C | - | - | Intergenic 855/857 region |
| 122,491 | | | | T | T | T | T | **C** | **C** | - | Partial deleted of OriS of A489 |
| 122,507 | | | | A | A | A | A | A | **G** | - | Partial deleted of OriS of A489 |
| After 124,517 | | | | C | C | - | C | - | - | C | Homopolymer C region in promoter of US10 |
| After 125,572 | | | | AACCCC | AACCCC | AACCCC | **AA–CC** | **AA–CCC** | AACCCC | **CA—A** | Homopolymer C region 3′ end of sorf4/3 |
| After 126,830 | | | | - | - | - | - | - | - | **G** | Intergenic 3′ end of US2 |
| After 126,890 | | | | - | - | - | - | - | **A** | - | US2 frameshift after Leu215; 229 aa vs 217 aa |
| US | | | | | | | | | | | |
| 137,311 | | | | A | A | A | A | **C** | **C** | A | Intragenic synonymous substitution in US7 |

[a]Minority differences are in bold. Light shaded area indicates differences observed in hypothetic genes affected by ipac2 changes. The darker shaded area indicates differences observed in the 855/857 variable repeat region. Note that mutations in the inverted repeats are only listed once. GenBank accession #'s USDA MN = MN518177, USDA JN = JN542534, and A489 = KY423284.

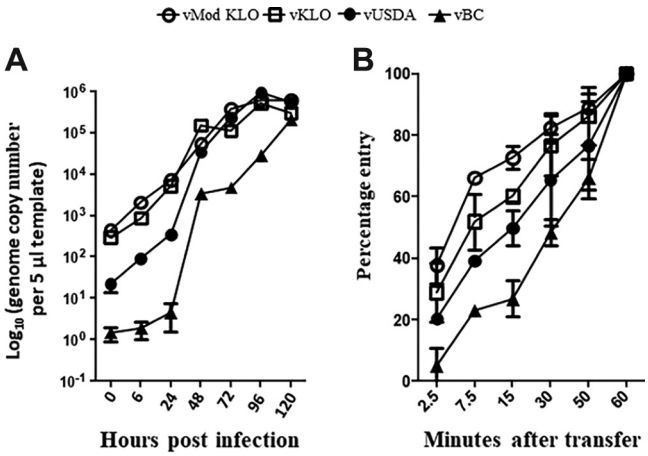


**FIG 6** *In vitro* replication kinetics. Virus growth (A) and entry kinetics (B) of vModKLO (open circles), vKLO (open squares), vBC (closed triangles), and the USDA reference strain (closed circles). vModKLO was reconstituted using the core cosmids pCIZ34, pCIS28, pCISB27, and pCIZ52 with YCp-ModKLO containing the GFP gene within the inverted ipac2 site. vKLO was reconstituted using the core cosmids and a YCp-KLO containing a linker in the ipac2 site. Reconstituted vBC was generated by transfecting YCp-BC with the core cosmids and contained no alterations. (A) LMH cell line cultures were inoculated at a multiplicity of infection (MOI) of 0.001, then the inocula were removed at 1 h postinoculation. Triplicate wells were harvested at 6 h, then at 24-h intervals after infection. Virus genome concentrations were determined in the cell-free supernatant by using qPCR. Error bars indicate standard deviations ($P > 0.05$). (B) Viral entry at different time points was calculated by contrasting the number of plaques formed after inoculation for that time period to the number of plaques formed after an inoculation period of 60 min (endpoint). The means and standard deviations (error bars) from 3 independent experiments are shown ($P > 0.05$).

high-quality DNA for cosmids pCISB27, pCIS28, pCIZ52, and the yeast/*E. coli* shuttle vectored recombinants.

To investigate this anomaly, the ipac2 site was targeted for mutagenesis, and 2 viable ipac2 mutants, vModKLO containing the marker gene GFP and vKLO containing a BamHI linker, were created via cotransfection of LHM cells. Since these mutants grew to high titers *in vitro* and were pathogenic in chickens, another virus recombinant (vBC) containing wildtype sequences with pac2 and ipac2 was generated for comparative purposes. Initially, the vBC recombinant and the control wildtype (USDA strain) appeared to grow slower than those infected with the Δipac2 recombinants vKLO and vModKLO, however, this was not statistically significant (*P* values between 0.7 and 0.1), especially at later times. The rates of entry were similar among the viruses. Although at early time points, recombinants lacking the ipac2 site appear slightly advantaged in entry, this was not statistically significant. Determining the plaque sizes of the recombinant viruses proved difficult due to the extreme fusogenic nature of ILTV when grown in LMH cells. To avoid bias in only selecting nearly round plaques, > 100 plaques were photographed (per virus) within 6-well dishes,

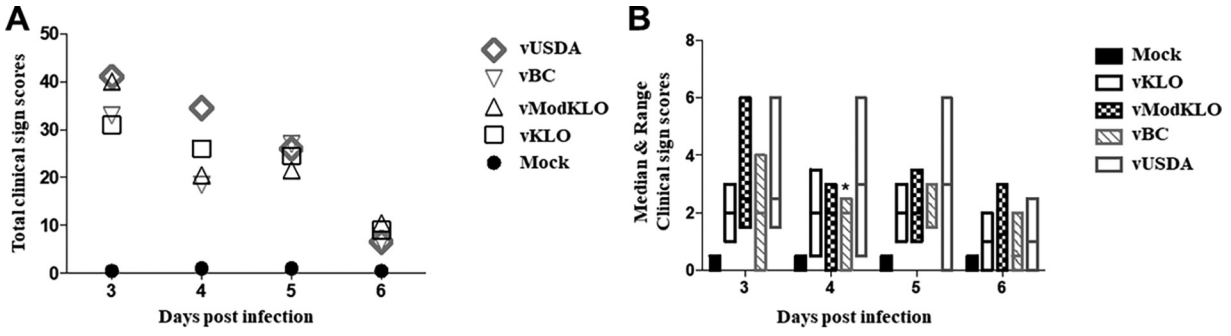


**FIG 7** Virulence evaluation of reconstituted ILTV recombinant compared to the USDA reference strain. SPF chickens were intratracheal-ocular inoculated with vModKLO, vKLO, vBC, and vUSDA or cell culture media (mock) at 21 days of age. (A) Total clinical sign scores for groups of chickens ($n = 10$) on days 3 to 6 are shown. (B) Median and range of clinical signs.

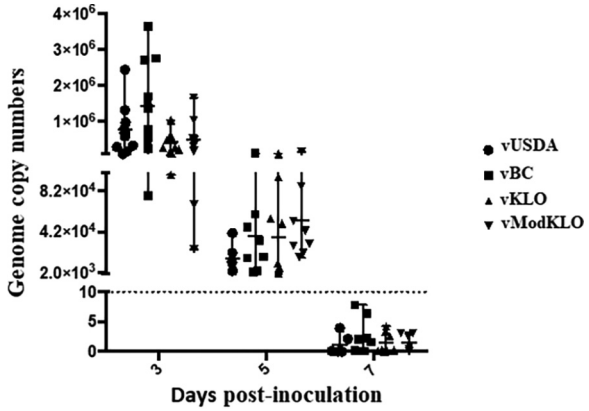


**FIG 8** Quantitation of viral load in the trachea at 3, 5, and 7 days post-ILTV inoculation. lltv genomes ($2^{-\Delta\Delta Ct}$)/tracheal swab as detected by duplex real-time PCR at various times after infection.

and the areas of outlined plaques were calculated. As shown in Fig. 5, a broad range of plaque diameters was obtained with no statistical difference in the sizes of the plaques.

Since viable viruses could be rescued from cosmid clones containing intact or deleted ipac2 sites, this region cannot be the culprit behind the difficulties in creating an ILTV BAC. Something else must be responsible for the instability of cosmid pCIZ34 and the problems in creating an infectious ILTV clone in *E. coli*. It has been previously reported that the palindromic structures constituting the origins of replication (OriL and OriS) of HSV-1 are unstable in *E. coli* (43, 44). Perhaps the origins of replications of ILTV, especially the OriL palindrome on cosmid pCIZ34, are unstable in *E. coli*. In experiments designed to piecemeal the inserts from the cosmids together to create a yeast-based infectious clone, we discovered that both the OriL and OriS sequences get deleted when the YCp DNA from these recombineered yeast clones are transferred to electrocompetent *E. coli* strains. This transfer of recombinant YCp shuttle vectors to *E. coli*. is routinely done for practical purposes since purification of YCps and YACs (yeast artificial chromosomes) from *S. cerevisiae* is arduous, with yields of only 5 $\mu$g per L culture (45, 46).

Unlike the origins of replication of HSV-1 (47), in which OriL is a 144 bp perfect palindrome and OriS is a 49 bp imperfect palindrome, both OriL and OriS of ILTV are exceptionally long perfect palindromic sequences of 268 bp and 280 bp, respectively. Only 4 nucleotides at the bubbles of each hairpin structure are unpaired. We have individually cloned the palindromic origins of replication of ILTV with flanking sequences (OriL and OriS, 879 and 717 bp, respectively) into the yeast shuttle vector pYES1L and have tried to transfer them into various strains of *E. coli* with no success. After PCR screening of hundreds of clones, no *E. coli* transformants that contained intact OriL or OriS sequences could be identified. Surprisingly, this screen also demonstrated that the OriS palindromes were missing in all of the YCp bridge recombinants (YCp-BC, YCp-KLO, and YCp-ModKLO). The OriS palindromes were intact following the assembly of these segments in yeast; however, upon transfer to electrocompetent *E. coli*, 203 bp of the palindromes were subsequently deleted. The nucleotide sequences of all recombinant cosmids, YCps (isolated from *E. coli*), and reconstituted viruses were determined to confirm these PCR results. Sequence analysis corroborated that the YCp bridge recombinants lacked the OriS palindromes, but interestingly, all sequenced reconstituted viruses (vBC, vKLO, and vModKLO) contained both copies (within the inverted repeats) of the intact OriS palindromes. This repair of the OriS palindrome within the terminal repeat through homologous recombination with cosmid pCIZ52 internal repeat sequences (containing an intact OriS) suggests that both OriL and OriS of ILTV are necessary for productive infection. We have yet to isolate viable ILTV recombinants with deletions in both copies of OriS using the cosmid/YCp-based system with intact OriS palindrome-containing pCIZ52 and ΔOriS bridge constructs. However, during the course of this research, an ILTV BAC was created and

unsurprisingly contained 215 bp deletions in both copies of the OriS palindromes (GenBank Accession # KY423284).

Although we have demonstrated that the OriS on pCIZ52 cosmid is stable after 10 serial passages in LB broth at 37°C using the PCR screen, it remains a mystery why the OriS palindrome on this cosmid is stable at all within *E. coli* strain XL Blue. We speculate that the unique tertiary structure of cosmid pCIZ52 is critical for preserving the palindrome's integrity and stability. This unique structure is not maintained in *E. coli* hosting YCp-cloned OriS palindromes or the KY423284 ILTV BAC containing the entire genome. Overall, *Escherichia coli* is a poor surrogate host for cloned ILTV genomic fragments.

In conclusion, the salient findings of this report are that: (i) Five cloned ILTV fragments can reconstitute viable virus upon transfection; (ii) the inverted pac2 site is nonessential for virus production; (iii) reconstituted recombinants are pathogenic in birds; (iv) recombinant viruses have *in vitro* growth and entry kinetics similar to wild-type virus; and (v) the origins of replication of ILTV are generally unstable in *E. coli*. The generation and characterization of recombinant viruses reported here represent the first example of infectious laryngotracheitis viruses solely created from molecularly cloned subgenomic fragments.

## MATERIALS AND METHODS

**Cells and viruses.** Leghorn male hepatoma (LMH) cells were grown in tissue culture dishes coated with 0.2% gelatin and propagated in Dulbecco's Modified Eagle Medium (DMEM) supplemented with 10 units/mL of penicillin, 10 $\mu$g/mL streptomycin, and 10% fetal bovine serum (FBS). Reconstituted ILTV was propagated on confluent monolayers of chicken kidney (CK) cells (48).

**Preparation of concatenated ILTV DNA and virion DNA.** CK cells were infected with the USDA strain of ILTV using a multiplicity of infection (MOI) of 0.01. Four days postinfection, the cells were harvested and processed using a modified Hirt supernatant procedure (49, 50). Briefly, cells were trypsinized, pelleted, and lysed at 37°C for 16 h in 1.0 mL (per 75cm2 of cells) in a buffer containing 50 mM Tris pH 8.0, 10 mM EDTA, 0.5% SDS, and 1 mg/mL of proteinase K (New England Biolabs). High molecular weight DNA was precipitated with 350 $\mu$L of a solution containing 3M CsCl, 1 M potassium acetate, and 0.67 M acetic acid. After centrifugation, the herpesvirus DNA was extracted thrice with phenol-chloroform and precipitated with ammonium acetate and ethanol.

To obtain enriched virion DNA, chicken kidney cell cultures were infected as above and harvested 7 days p.i., lysed by freeze-thawing, and centrifuged for 10 min at 4000 rpm. Next, the supernatant was transferred to SW32 ultracentrifuge tubes, underlaid with 5 mL 30% sucrose in PBS, and centrifuged for 2 h at 20,000 rpm and 4°C. Then, the supernatant was completely aspirated, the pellet was washed once with TEN buffer, sedimented again for 1 h at 20,000 rpm, and resuspended in TEN buffer for DNA preparation, as described previously (51).

**Construction of recombinant DNA.** A pathogenic isolate of ILTV (obtained from D. Lűtticken, Boxmeer, NL) was used to construct the overlapping cosmid clones pCIZ34, pCIS28, pCISB27, and pCIZ52. ILT virion DNA was partially digested with Sau3AI, and fragments ranging from approximately 30 to 50 kbp were isolated from 0.6% agarose gels using diethylaminioethyl (DEAE) cellulose membranes (52) and cloned into the BamHI site of pSuperCos according to the instructions supplied by Stratagene (now Agilent). Ligated inserts were packaged using Gigapack gold packaging extracts, diluted in SM buffer (100 mM NaCl, 8 mM MgSO4 ·7H2O, 50 mM Tris-HCl, pH 7.5, and 0.01% gelatin), and used to infect XL1-Blue MR *E. coli*. Antibiotic-resistant clones were selected on LB agar plates supplemented with 0.2% (vol/vol) maltose, 10M MgSO4, and 100 $\mu$g/mL ampicillin. Mini prep DNA was subjected to restriction endonuclease profiling. Additional clones (pBC-114, pKLO-26, and pModKLO-10) spanning the $TR_S$/UL junction were generated with PCR products ligated into pUC19 using Gibson Assembly fusion cloning (New England Biolabs). The primers used in amplification reactions to generate PCR products are listed in Table 3.

To construct the pBC-114 clone containing one pac1 site and two pac2 sites (wild type configuration), primers "For3'TRS ILTV" and "REV5'UL ILTV" were used along with ILTV Hirt supernatant DNA (62 ng) to generate a 3,221 bp PCR product. Plasmid pUC19 was used as a template to generate a 2,712 bp PCR product using the primer pairs "For pUC19 04202014" and "REV pUC19 04202014" and 50 ng of pUC19. The fragments were amplified using Platinum Pfx polymerase (Invitrogen) in a buffer containing 2 mM MgSO4 with the following amplification parameters. After denaturing the templates at 94°C for 2 min, the parameters for 40 cycles were: 94°C for 30 s, annealing at 62°C for 30 s, and extension at 68°C for 2 min, respectively, followed by a final extension at 68°C for 15 min. These conditions were used for both amplification reactions.

These amplification reagents and conditions were also used to generate pKLO-26 and pModKLO. The pKLO-26 clone containing the deletion in the downstream ipac2 site was created using Gibson Assembly fusion cloning with 2 inserts that were generated in pfx polymerase amplification reactions with the 2 primer pairs ("For3' TRS ILTV" and "REV PAC2 ILTV") ("For PAC2 ILTV" and "REV5'UL ILTV") and 62 ng of ILTV Hirt supernatant DNA. These 1,896 bp L and 1,282 bp O fragments were ligated with the 2,712 bp pUC19 PCR product. Fusion cloning was also used to generate the pModKLO clone in which the downstream ipac2 site was replaced with a GFP/kanamycin cassette. Two inserts were generated with the 2 primer pairs ("*MluI* FOR KLO" and "*BsrG*I REV KLO") ("*Asi*SI FOR KLO" and "*EcoRI* REV KLO") and 62 ng of ILTV Hirt supernatant DNA. The sizes of the PCR products were 1,989 and 1,293 bp, respectively.

**TABLE 3** Oligonucleotides used in the construction of the recombinants

| Primer name | Sequence |
|---|---|
| For pUC19 04202014 | CTTCCCAGCGGCCGGTATTCCTAACCATGGAATTCACTGGCCGTCGTTTTACAACGTCG |
| REV pUC19 04202014 | GGCTCTAGTGTAGCCGCTTCCGGGTATAGTCTGCAGGCATGCAAGCTTGGCGTAATCATG |
| FoR PAC2 ILTV | GCTGCAATGACTTCCTGATTTAATGGATCCAGGATCAGAGACCGCCTCCAATCCCT |
| REV 5′UL ILTV | CGACGTTGTAAAACGACGGCCAGTGAATTCCATGGTTAGGAATACCGGCCGCTGGGAAG |
| For 3′TRS ILTV | CATGATTACGCCAAGCTTGCATGCCTGCAGACTATACCCGGAAGCGGCTACACTAGAGCC |
| REV PAC2 ILTV | AGGGATTGGAGGCGGTCTCTGATCCTGGATCCATTAAATCAGGAAGTCATTGCAGCCTGC |
| For 3′TRS ILTV | CATGATTACGCCAAGCTTGCATGCCTGCAGACTATACCCGGAAGCGGCTACACTAGAGCC |
| REV 5′UL ILTV | CGACGTTGTAAAACGACGGCCAGTGAATTCCATGGTTAGGAATACCGGCCGCTGGGAAG |
| *Mlu*I FOR KLO | ATGACCATGATTACGCCAAGCTTGCATGCACGCGTACTATACCCGGAAGCGGCTACACTA |
| *BsrG*I REV KLO | CGCGCACATTTCCCCGAAAAGTGCTGTACAATTAAATCAGGAAGTCATTGCAGCCTGcaa |
| *BsrG*I Fill KLO | TTGCAGGCTGCAATGACTTCCTGATTTAATTGTACAGCACTTTTCGGGGAAATGTGCGCG |
| *As i*SI REV KLO | GAGGGATTGGAGGCGGTCTCTGATCCGCGATCGCGTGTTTGTGTGTTTGTGGAGCAGCAT |
| *Asi*SI FOR KLO | ATGCTGCTCCACAAACACACAAACACGCGATCGCGGATCAGAGACCGCCTCCAATCCCTC |
| *EcoR*I REV KLO | CCAGTCACGACGTTGTAAAACGACGGCCAGTGAATTCCATGGTTAGGAATACCGGCCGCT |
| *EcoR*I FOR KLO | CTTCCCAGCGGCCGGTATTCCTAACCATGGAATTCACTGGCCGTCGTTTTACAACGTCGT |
| *Mlu*I REV KLO | TCTAGTGTAGCCGCTTCCGGGTATAGTACGCGTGCATGCAAGCTTGGCGTAATCATGGTC |
| ILTV *BsrG*I For | ATATGTACAGAACGACCGAGCGCAGCGGCGGCCGCGCTGATACCGCCGCTTAATTAAGCTCTTCGCCTAACTATTGCTTTCATGATTTA |
| ILTV *Spe*I REV | TTTACTAGTCGCATTCCCTGCGGAAAGAC |
| Linker 2 FW rep2 | TTCTTGACCTCTCTTTCGGCCGTCACAGTATCTTCTGGATCCTCGCCGCAGTTAATTAAAGTCAGTGAGCGAGGAAGCGC |
| Linker 2 RV rep2 | GCGCTTCCTCGCTCACTGACTTTAATTAACTGCGGCGAGGATCCAGAAGATACTGTGACGGCCGAAAGAGAGGTCAAGAA |
| R3_14KB | CTTCCCGATCACATTCAGG |
| 14Kb_1922_F | CAACGTATGTCGGTTGGTTG |
| OriS FW1 | GAACGACCGAGCGCAGCGGCGGCCGCGCTGATACCGCCGCCTTCCCGATCACATTCAGGGTCGGGGGTCGAGGGGGGTGC |
| OriL RV1 | GCACCCCCCTCGACCCCCGACCCTGAATGTGATCGGGAAGGCGGCGGTATCAGCGCGGCCGCCGCTGCGCTCGGTCGTTC |
| OriS_FW2 | AAGTGATATTAGGACATAGTCAACCAACCGACATACGTTGCCTCGCCGCAGTTAATTAAAGTCAGTGAGCGAGGAAGCGC |
| OriS_RV2 | GCGCTTCCTCGCTCACTGACTTTAATTAACTGCGGCGAGGCAACGTATGTCGGTTGGTTGACTATGTCCTAATATCACTT |
| cos 34 seq 87F | GCGCTGCACGCTCGAATTTTAA |
| cos34 Rev1 | CAAAAATCTCGATTGACATCCTG |
| OriL_FW1 | GAACGACCGAGCGCAGCGGCGGCCGCGCTGATACCGCCGCGCGCTGCACGCTCGAATTTTAAAAAGAACAAATGTCATTT |
| OrL_RV1 | AAATGACATTTGTTCTTTTTAAAATTCGAGCGTGCAGCGCGCGGCGGTATCAGCGCGGCCGCCGCTGCGCTCGGTCGTTC |
| OriL_FW2 | TGGGGCGGCACATCCGGCAGGATGTCAATCGAGATTTTTGCCTCGCCGCAGTTAATTAAAGTCAGTGAGCGAGGAAGCGC |
| OriL_RV2 | GCGCTTCCTCGCTCACTGACTTTAATTAACTGCGGCGAGGCAAAAATCTCGATTGACATCCTGCCGGATGTGCCGCCCCA |

The third insert was generated with the primer pair ("*BsrG*I For KLO" and "*AsiS*I REV KLO") with 100 ng of DNA isolated from the GΔORFC virus (53) and yielded a 3,979 bp product containing the GFP/kanamycin cassette. The pUC19 vector component was amplified using the primers pair ("*EcoRI* FOR KLO" and "MluI REV KLO") with 50 ng of pUC19 DNA to generate a 2,709 bp PCR product. All fusion cloning procedures were performed with a 2-fold molar excess of inserts relative to the vector in a 20 $\mu$L reaction mixture for 30 min at 50°C. *E. coli* DH5$\alpha$ cells were transformed with the ligation products from all of the Gibson ligation experiments and propagated on Luria-Bertani (LB) plates containing 100 $\mu$g/mL of carbenicillin.

**Yeast genetic assembly of $U_S$-$TR_S$-UL and origin of replication (OriL and OriS) clones.** Constructs (YCp-BC, YCp-KLO, and YCp-ModKLO) containing 2.0 Kb segment from the 3′ end of the $U_S$, the complete 14.5 Kb $TR_S$ sequences and variants of the 5′ UL sequences with or without alteration in the ipac2 site were assembled using the GeneArt High-Order Genetic Assembly System (Invitrogen) with PCR products and restriction endonuclease fragments from cosmid pCIZ52 and the pYes1L vector. A 5.1 Kb PCR product spanning the $U_S$/$TR_S$ junction was amplified using the primer pairs ("ILTV *BsrG*I For" and "ILTV *SpeI* REV") and 100 ng of GΔORFC virus (53), digested with BsrGI and SpeI and cloned into the synthetic minigene (MiniRepair -pIDT-SMART-AMP) to generate the recombinant pFX5.1. Cosmid pCIZ52 was digested with EcoRV, SpeI, AseI, and KpnI, and a 13.9 Kb KpnI–SpeI fragment was excised and used in assembly reactions with the oligonucleotide "stitches" ("Linker 2 FW rep2" and "Linker 2 RV rep2"). Likewise, the BsrGI-SpeI insert was gel purified from digested pFX5.1. Three assembly reactions were performed that contained the common fragments 5.1 Kb BsrGI- SpeI fragment and the 13.9 Kb KpnI-SpeI RE fragment, with either the 6.9 Kb MluI-EcoRV ModKLO fragment, the 3.0 Kb PstI-EcoRV KLO fragment or the 3.1 Kb PstI-EcoRV BC fragment.

PCR products containing the origins of replication were also cloned using the GeneArt High-Order Genetic Assembly System. The OriS and OriL fragments of ILTV were generated using primers "R2_14Kb" and "14Kb_1922F" and primers "cos 34 seq 87 F" and "cos34 Rev" with 50 ng of cosmid template pCIZ52 or pCIZ34, respectively. The amplification reaction conditions were as described above with similar cycling parameters, except the extension time was reduced to 1 min. The OriS PCR product (876 bp) was recombineered into the vector pYES1L using the stitching oligonucleotides OriS_FW1/OriS_RW1 and OriS_FW2/OriS_RVs to generate YCp-OriS. Similarly, the OriL PCR product (717 bp) was cloned using stitching oligonucleotides OriL_FW1/OriL_RW1 and OriL_FW2/OriL_RV2 to generate YCp-OriL.

All the assemblies of PCR products and restriction endonuclease fragments were performed in yeast (strain MaV203) using the PEG/lithium acetate transformation procedure with 100 ng of pYES1L vector,

200 ng of each insert, and 20 pmol of stitching oligonucleotides. Yeast transformants were selected on minimal yeast plates without tryptophan and screened using yeast colony PCR. Colonies were lysed in 50 $\mu$L of water with 2.5 Units of Lyticase (Millipore-Sigma) for 30 min at 37°C. DNA was released from spheroplasts by heating the solution to 95°C for 10 min, and 1.25 $\mu$L was used in a standard 12.5 $\mu$L PCR with HotStart *Taq* polymerase (New England Biolabs). Positive transformants from the PCR screens were propagated overnight at 30°C in yeast media (YPD) without tryptophan. DNA was isolated using a Zymolyase mini prep procedure and used to transform electrocompetent *E. coli* (TOP10) to generate recombinants YCp-ModKLO, YCp-KLO, and YCp-BC. *E. coli* recombinants were propagated in LB broth containing 50 $\mu$g/mL of spectinomycin. Miniprep DNA was isolated using alkaline lysis without phenol-chloroform extractions and characterized with restriction digestions.

Common electrocompetent strains from New England Biolabs (DH10$\beta$, NEB 5$\alpha$), ThermoFisher (TOP10), and Agilent (XL-1 Blue) were initially used to test whether they would be suitable hosts for the stable propagation of YCp-OriS and YCp-OriL. Briefly, transformed yeast cells were screened for intact OriL and OriS palindrome using the lyticase PCR procedure. The mini prep DNA (100 ng) from positive yeast colonies was first treated with Exonuclease V (Plasmid Safe, Lucigen), then used to transform the various electrocompetent cells. Next, recombinants were selected on LB plates containing 50 $\mu$g/mL spectinomycin. Finally, *E. coli* recombinants were again screened for the intact origin of replication using the *E. coli* colony PCR procedure.

The electrocompetent *E. coli* strains 6262, 6786, and 6787 from Scarab Genomics were also tested for their usefulness in the stable propagation of the origin palindromes. The transformation protocol was identical to the above fore-mentioned, except the recombinants were selected on agar plates containing Modified Korz Medium with Glucose supplemented with 100 $\mu$g/mL of spectinomycin (54).

**Conversion of ILTV cosmids to YCps.** A mini gene was synthesized (IDT DNA technologies) that contained short DNA sequences necessary for homologous recombination with pSuperCos vector sequences that flanked the ILTV genomic inserts. Specifically, DNA block 1 contained 151 bp of sequence homologous to those 5′ of the T7 primer binding site, and block M had 157 bp of sequence homologous to those found immediately downstream of the Amp resistance ORF in pSuperCos. These DNA blocks, which contain a unique BamHI restriction endonuclease site between them, were cloned into pYES1L using standard cloning procedures with NotI and PacI. The final construct, linearized with BamHI, was used in assembly reactions with SfiI-linearized pCIZ34, pCISB27, pCIS28, and pCIZ52 (partially digested). All assemblies were performed in yeast (strain MaV203) using the PEG/lithium acetate transformation procedure as previously stated. *E. coli* TOP10 (ThermoFisher) was transformed with mini prep DNA isolated from yeast colonies and selected on LB plates containing 100 $\mu$g/mL ampicillin. *E .coli* recombinants were screened using colony PCR with the origin of replication-flanking primers, and miniprep DNA was characterized using restriction digestion.

**Sequencing.** The nucleotide sequences of the cosmids were determined using the Illumina MiSeq platform. Paired-end library preparation was performed by standard Illumina methods. Briefly, each sample was sheared, size-fractionated to 500 bp in length, and ligated to Illumina adapters with a unique barcode per sample. Each library was generated using the Illumina TruSeq Nano LT Sample Preparation Kit, according to the manufacturer's specifications. The quantity and quality of the DNA were assessed using the Qubit BR dsDNA assay (Invitrogen) and an Agilent DNA High Sensitivity series chip assay. Libraries were standardized to 2 nM, and paired-end sequencing was performed on an Illumina MiSeq using version 2 kits to generate ca. 1 to 3 million 150 nuc paired-end reads per sample. Residual adapter-containing reads were removed, and reads were trimmed from the 3′ to a median Phred score of 30 and a minimum length of 50 nucleotides. The sequences of the $U_S$-$TR_S$-UL clones (BC-114, KLO-26, and ModKLO-10), and the origin of replication clones (YCp-OriS and YCp-OriL) were determined using Sanger sequencing with custom oligonucleotides. The genomic coordinates of the cosmid and YCp inserts are presented in Table 1.

**Sequence assembly.** Read preprocessing and assembly were performed using workflows run with Nextflow v18.10.1.5003 (55). Briefly, raw reads were quality-checked using FastQC v0.11.7 (56) and trimmed using Trim Galore v0.4.5 (57) (minimum quality = 8, minimum trimmed length = 40, stringency = 4). Host sequence removal was performed using the BBDuk tool of the BBTools package v.38.06 (58) (k = 35, hdist = 0). Digital normalization was performed using the BBNorm tool from BBTools (tgtcov = 75, minabund = 4, fixspikes=t). De novo assembly was performed using MIRA v4.9.6 (59) (parameter file available upon request). Circularization was performed using a modified Minimus2 script (60) from the AMOS package. Manual finishing was performed using Staden Gap5 v2.0.0b11 (61). Annotation was performed using an in-house avian herpesvirus-specific pipeline.

**Generation of viruses from cosmid and yeast centromeric plasmid clones.** DNA was purified from 500 mL cultures (LB medium plus 100 $\mu$g/mL of ampicillin [cosmids] or 50 $\mu$g/mL spectinomycin [YCp]) using Nucleobond BAC100 (TaKaRa Bio). To facilitate homologous recombination, the cosmid, and YCp recombinants were digested with restriction endonucleases. The restriction endonuclease PacI was used to linearize the $TR_S$/UL clone YCp-ModKLO. NotI was used to linearize cosmid clones pCIZ34 and pCISB27. Cosmids pCIS28 and pCIZ52 were linearized with restriction endonucleases *Asc*I and PacI. Clones YCp-KLO and YCp-BC were digested with PacI and SwaI, respectively. The DNA was subjected to microdialysis and concentrated via vacuum centrifugation after heat inactivation of the restriction endonucleases. The DNA concentrations were measured using a Qubit mini fluorometer (Invitrogen). Equimolar amounts (50 femtomoles) of the 4 digested cosmids (pCIZ34, pCIS28, pCISB27, and pCIZ52) and YCp recombinants (either YCp-BC, YCp-KLO, or YCp-ModKLO) with 2.0 $\mu$g of ancillary expression plasmids encoding ILTV $U_L$48 and ICP4 were mixed with 12 $\mu$L of Mirus TransIT-LT1 reagent in 250 $\mu$L of serum-free medium. After a 30-minute incubation, the DNA- lipid complexes were added to semi-confluent monolayers of LMH cells. Transfected cells were incubated at 37°C under 5% CO2 and monitored daily for signs of cytopathic effect (CPE). CPE was observed on day 5, and whole-cell freezer preps were made on day 6 posttransfection. Briefly, the medium containing cell-free ILTV was removed and stored at −80°C. The infected cells (with 500 $\mu$L of

medium) were also stored at −80°C and subjected to 3 rounds of freeze-thaw cycles to release the cell-associated virus. The stability of the reconstituted ILTV recombinants was investigated by sequential passage (3 times) in monolayers of CK cells. The rescued viruses were allowed to infect subconfluent monolayers of CK cells for 16 h, after which the medium was replaced with fresh medium, and the infection was allowed to proceed for an additional 5 days. The supernatants were removed, and both the supernatants and infected cells (with 1.0 mL of medium) were frozen at −80°C. Following thawing, cell scrapers were used to disrupt the infected monolayer. After an additional freeze/thaw cycle, the cells were pelleted at 350 × *g* for 10 min. Freshly prepared CK cells were then infected with dilutions of these cell-free virus preparations. Virus stocks of the USDA reference strain of ILTV and viruses generated from cosmids/YCp recombinants were obtained by infecting CK cells with a MOI of 0.001. After 6 dpi, the infected cells were harvested, followed by 3 cycles of freeze/thawing and titered (see below).

**Plaque size assay, growth, and entry kinetics of reconstituted viruses.** The replication properties and spread of the reconstituted vBC, vKLO, vModKLO, and the USDA strain were analyzed in LMH cells. Briefly, LMH cells were seeded into 0.2% gelatin-treated 6-well plates, 5 × 105 cells in 3.0 mL of DMEM containing 10% FBS and antibiotics, and incubated at 39°C for 24 h. The medium was then removed, and the cells were inoculated with the recombinants or the USDA reference strain (MOI of 0.001). Viruses were absorbed for 60 min at 39°C. For the plaquing essay, the inoculum was removed after absorption, and the cells were rinsed once with media and overlaid with 1% wt/vol methylcellulose in DMEM, with 10% FBS, 50 $\mu$g/mL ampicillin, and 50 $\mu$g/mL gentamicin. Cells were incubated at 39°C for 5 days, fixed with 4% paraformaldehyde, and stained with 1% crystal violet (CV) in 20% ethanol and dH2O. All plaques were photographed from 6-well dishes, the plaque areas were outlined manually, and the areas were measured using ImageJ Fiji (https://imagej.net/software/fiji/downloads). Plaque diameters were determined from area calculations and compared to those obtained with USDA ILTV reference control. For the growth kinetics experiments, cells were infected with the same MOI of 0.001, and supernatants from 3 independent wells of each virus were collected at 0, 6, 24, 48, 72, 96, and 120 h postinoculation for qPCR measurements. Virus titers were determined in LMH and CK cells and expressed as the mean $\log_{10}$ TCID50 mL-1. The vBC, vKLO, and vModKLO recombinant viruses and the USDA strain utilized in the animal experiments were propagated and titered in CK cells. For the viral entry kinetics, after 60 min at 39°C virus adsorption, infected LMH cell monolayers were covered with methyl-cellulose overlay media (1% wt/vol methylcellulose in DMEM, with 10% FBS, 50 $\mu$g/mL ampicillin, and 50 $\mu$g/mL gentamicin), and the number of plaques formed after inoculation (2.5, 7.5, 15, 30, and and 50 min) was compared to the number of plaques formed after an inoculation period of 60 min (endpoint). Copy numbers per 5 $\mu$L template were determined using Real-time qPCR as previously described (62). Further details on the *in vitro* multi-step virus growth and entry kinetics can be found in Devlin et al. (63) and Lee et al. (64).

**Animal pathogenicity study.** The objective of the first experiment was to determine the virulence of the 3 reconstituted viruses in specific pathogen-free (SPF) chickens compared to the USDA ILTV reference strain. Briefly, 75 1-day-old SPF chickens (Merial Select) were distributed into 5 groups of 15 birds and placed in colony houses (Poultry Diagnostic Research Center, Athens, GA). At 3 weeks of age, 4 of the 5 groups were inoculated intratracheally (100 $\mu$L) and in the eye conjunctiva (50 $\mu$L each eye) with a dose of 3.5 ($\log_{10}$) TCID50 per chicken of the vBC, vKLO, and vModKLO recombinants or the USDA strain. The remaining 15 chickens were mock-inoculated with tissue culture media. On days 3, 5, and 7 postinoculation, tracheal swabs were collected from each group of chickens and analyzed by real-time PCR to determine the trachea virus load.

**Clinical sign and mortality scores.** Clinical signs of conjunctivitis, respiratory distress, lethargy, and mortality were scored from days 3 to 6 postinoculation as described by Vagnozzi et al. (65). Clinical sign categories of conjunctivitis, respiratory distress, and lethargy were evaluated in individual chickens and given a score. No clinical signs were given a score of 0; mild, a score of 1; moderate, a score of 2; and severe, a score of 3. In the case of mortality, a score of 6 was given. Each chicken received a total clinical sign score, and a mean clinical sign score was calculated at each time point. At the time point where the peak of the clinical signs was observed, the median clinical sign score for each group was compared.

**DNA extraction of tracheal *aspirates*.** Tracheal swabs were placed in 2 mL tubes containing 1X PBS solution with 2% antibiotic-antimycotic (100X, Invitrogen) and 2% newborn calf serum. Swabs were stored at −80°C until processed. Viral DNA extraction from tracheal samples was performed using the MagaZorbH DNA mini prep 96-well kit (Promega), as described by Johnson et al. (66).

**Quantitative real-time PCR for ILTV in tracheal swabs.** The ILTV viral load in each of the tracheal swab samples was quantified by real-time PCR (qPCR) in a duplex assay normalized to a host gene as described by Vagnozzi et al. (67). The amount of ILTV DNA was measured by the qPCR assay on an Applied Biosystems 7500 Fast real-time PCR system (Life Technologies) with specific primers and probes of the $U_L44$ gene of ILTV (encoding glycoprotein C) and the endogenous control gene (avian $\alpha$2-collagen gene) as described previously (68). Briefly, the duplex reactions for ILTV were set up to a final volume of 25 $\mu$L as follows: 12.5 $\mu$L of 2x master mix (TaqMan universal master mix II with UNG, Applied Biosystems), 1.25 $\mu$L of collagen primers to a final concentration of 0.5 $\mu$M, 1.25 $\mu$L of ILTV primers to a final concentration of 0.5 $\mu$M, 1.25 $\mu$L probes to a final concentration of 0.1 $\mu$M, and 5 $\mu$L of DNA template. In both PCR methods, the thermal cycling profile used was 50°C for 2 min, 95°C for 10 min, and 40 cycles of 95°C for 15 s and 60°C for 60 sec. The relative amount of ILTV genomes detected per sample was expressed as the $\log_{10}$ 2-ΔΔCt (67, 69).

**Statistical analysis.** Plaque size data of ILTV recombinant viruses were analyzed as plaque diameters using one-way analysis of variance (ANOVA), with Bonferroni correction for multiple comparison in the case of a *P* value of $<0.01$. The two-way ANOVA was utilized to highlight differences in mean viral titers of vBC, vKLO, vModKLO, and its parental USDA strain when grown in LMH cells. Genome copy numbers were compared at 0, 24, 48, 72, 96, and 120 h postinoculation *in vitro*. Error bars indicate SD from 3

replicates. $P$ values $< 0.05$ were considered significant. The one-way ANOVA Kruskal–Wallis test ($P < 0.05$) was used to highlight differences in: (i) median clinical signs scores among groups of chickens inoculated via the intratracheal route with vBC, vKLO, vModKLO, and the USDA strain; (ii) mean viral genome load in trachea from chickens that received the recombinants and the USDA strain via the intratracheal-ocular route. Statistical analysis was performed using GraphPad PRISM 6.0 software (GraphPad Software).

**Animal experiments.** All animal experiments described in this study were performed under the Animal Use Protocol AUP A2016-10-010-Y2-A2 approved by the Animal Care and Use Committee (IACUC) in accordance with regulations of the Office of the Vice President for Research at the University of Georgia.

## ACKNOWLEDGMENTS

We thank Laszlo Zsak and John Dunn for advice and continued support during this project. We thank Keith Jarosinski for his critical review of this manuscript. Mention of trade names or commercial products in this publication is solely to provide specific information and does not imply recommendation or endorsement by the U.S. Department of Agriculture. This work was supported by USDA-ARS CRIS project number 6040-32000-074-00D.

## REFERENCES

1. Anonymous. June 16, 2015. Infectious laryngotracheitis (ILT). http://www.canadianpoultry.ca. Accessed
2. Bagust TJ, Jones RC, Guy JS. 2000. Avian infectious laryngotracheitis. Rev Sci Tech 19:483–492. https://doi.org/10.20506/rst.19.2.1229.
3. Davison AJ. 2010. Herpesvirus systematics. Vet Microbiol 143:52–69. https://doi.org/10.1016/j.vetmic.2010.02.014.
4. Fuchs W, Veits J, Helferich D, Granzow H, Teifke JP, Mettenleiter TC. 2007. Molecular biology of avian infectious laryngotracheitis virus. Vet Res 38:261–279. https://doi.org/10.1051/vetres:200657.
5. Kotiw M, Sheppard M, May JT, Wilks CR. 1986. Differentiation between virulent and avirulent strains of infectious laryngotracheitis virus by DNA: DNA hybridization using a cloned DNA marker. Vet Microbiol 11:319–330. https://doi.org/10.1016/0378-1135(86)90062-3.
6. Kotiw M, Wilks CR, May JT. 1982. Differentiation of infectious laryngotracheitis virus strains using restriction endonucleases. Avian Dis 26:718–731. https://doi.org/10.2307/1589858.
7. Garcia M, Spatz S, Guy JS. 2013. Infectious laryngotracheitis. *In* Swayne DE, Glisson JR, McDougald LR, Nolan LK, Suarez DL, Nair V (ed), Diseases of poultry, vol 13th edition. Wiley-Blackwell, Ames, IA.
8. Volkening JD, Spatz SJ. 2013. Identification and characterization of the genomic termini and cleavage/packaging signals of gallis herpesvirus type 2. Avian Diseases 57:401–408. https://doi.org/10.1637/10410-100312-Reg.1.
9. Ziemann K, Mettenleiter TC, Fuchs W. 1998. Gene arrangement within the unique long genome region of infectious laryngotracheitis virus is distinct from that of other alphaherpesviruses. J Virol 72:847–852. https://doi.org/10.1128/JVI.72.1.847-852.1998.
10. Camp HS, Coussens PM, Silva RF. 1991. Cloning, sequencing, and functional analysis of a Marek's disease virus origin of DNA replication. J Virol 65:6320–6324. https://doi.org/10.1128/JVI.65.11.6320-6324.1991.
11. Gelenczei E, Marty E. 1962. Strain stability and immunologic characteristics of tissue-culture modified infectious laryngotracheitis virus. Avian Dis 9:44–56.
12. Samberg Y, Aronovici I. 1969. The development of a vaccine against avian infectious laryngotracheitis. I. Modification of a laryngotracheitis virus. Refu Vet 26:54–59.
13. Esaki M, Noland L, Eddins T, Godoy A, Saeki S, Saitoh S, Yasuda A, Dorsey KM. 2013. Safety and efficacy of a turkey herpesvirus vector laryngotracheitis vaccine for chickens. Avian Dis 57:192–198. https://doi.org/10.1637/10383-092412-Reg.1.
14. Gimeno IM, Cortes AL, Guy JS, Turpin E, Williams C. 2011. Replication of recombinant herpesvirus of turkey expressing genes of infectious laryngotracheitis virus in specific pathogen free and broiler chickens following in ovo and subcutaneous vaccination. Avian Pathol 40:395–403. https://doi.org/10.1080/03079457.2011.588196.
15. Maekawa D, Beltran G, Riblet SM, Garcia M. 2019. Protection efficacy of a recombinant herpesvirus of turkey vaccine against infectious laryngotracheitis virus administered In ovo to broilers at three standardized doses. Avian Dis 63:351–358. https://doi.org/10.1637/12029-011119-Reg.1.
16. Garcia M, Zavala G. 2019. Commercial vaccines and vaccination strategies against infectious laryngotracheitis: what we have learned and knowledge gaps that remain. Avian Dis 63:325–334. https://doi.org/10.1637/11967-090218-Review.1.
17. Palomino-Tapia VA, Zavala G, Cheng S, Garcia M. 2019. Long-term protection against a virulent field isolate of infectious laryngotracheitis virus induced by inactivated, recombinant, and modified live virus vaccines in commercial layers. Avian Pathol 48:209–220. https://doi.org/10.1080/03079457.2019.1568389.
18. Schadler J, Sigrist B, Meier SM, Albini S, Wolfrum N. 2019. Virus-like particles in a new vaccination approach against infectious laryngotracheitis. J Gen Virol 100:1013–1026. https://doi.org/10.1099/jgv.0.001272.
19. Kotiw M, Wilks CR, May JT. 1995. The effect of serial *in vivo* passage on the expression of virulence and DNA stability of an infectious laryngotracheitis virus strain of low virulence. Vet Microbiol 45:71–80. https://doi.org/10.1016/0378-1135(94)00115-D.
20. Guy JS, Barnes HJ, Smith L. 1991. Increased virulence of modified-live infectious laryngotracheitis vaccine virus following bird-to-bird passage. Avian Dis 35:348–355.
21. Hughes CS, Williams RA, Gaskell RM, Jordan FT, Bradbury JM, Bennett M, Jones RC. 1991. Latency and reactivation of infectious laryngotracheitis vaccine virus. Arch Virol 121:213–218. https://doi.org/10.1007/BF01316755.
22. García M, Spatz S. 2020. Infectious laryngotracheitis, p 189–209. *In* Swayne DE, Boulianne M, Logue CM, McDougald LR, Nair V, Suarez DL, de Wit S, Grimes T, Johnson D, Kromm M, Prajitno TY, Rubinoff I, Zavala G. (ed), Diseases of poultry. Wiley, Hoboken, NJ.
23. Korsa MG, Devlin JM, Hartley CA, Browning GF, Coppo MJC, Quinteros JA, Loncoman CA, Onasanya AE, Thilakarathne D, Diaz-Mendez A. 2018. Determination of the minimum protective dose of a glycoprotein-G-deficient infectious laryngotracheitis virus vaccine delivered via eye-drop to week-old chickens. PLoS One 13:e0207611. https://doi.org/10.1371/journal.pone.0207611.
24. Bilge-Dagalp S, Farzani TA, Dogan F, Akkutay Yoldar Z, Ozkul A, Alkan F, Donofrio G. 2021. Development of a BoHV-4 viral vector expressing tgD of BoHV-1 and evaluation of its immunogenicity in mouse model. Braz J Microbiol 52:1119–1133. https://doi.org/10.1007/s42770-021-00525-z.
25. Donofrio G, Martignani E, Sartori C, Vanderplasschen A, Cavirani S, Flammini CF, Gillet L. 2007. Generation of a transposon insertion mutant library for bovine herpesvirus 4 cloned as a bacterial artificial chromosome by in vitro MuA based DNA transposition system. J Virol Methods 141:63–70. https://doi.org/10.1016/j.jviromet.2006.11.028.
26. Fukuhara H, Ino Y, Kuroda T, Martuza RL, Todo T. 2005. Triple gene-deleted oncolytic herpes simplex virus vector double-armed with interleukin 18 and soluble B7-1 constructed by bacterial artificial chromosome-mediated system. Cancer Res 65:10663–10668. https://doi.org/10.1158/0008-5472.CAN-05-2534.
27. Fukuhara H, Takeshima Y, Todo T. 2021. Triple-mutated oncolytic herpes virus for treating both fast- and slow-growing tumors. Cancer Sci 112:3293–3301. https://doi.org/10.1111/cas.14981.
28. Kim T, Spatz SJ, Dunn JR. 2020. Vaccinal efficacy of molecularly cloned Gallid alphaherpesvirus 3 strain 301B/1 against very virulent Marek's disease virus challenge. J Gen Virol 101:542–552. https://doi.org/10.1099/jgv.0.001403.

29. Lee Y, Maes RK, Kruger JM, Kiupel M, Giessler KS, Soboll HG. 2021. Safety and efficacy of felid herpesvirus-1 deletion mutants in cats. Viruses 13. https://doi.org/10.3390/v13020163.
30. Liao Y, Bajwa K, Reddy SM, Lupiani B. 2021. Methods for the manipulation of herpesvirus genome and the application to Marek's disease virus research. Microorganisms 9:1260. https://doi.org/10.3390/microorganisms9061260.
31. Muniraju M, Mutsvunguma LZ, Foley J, Escalante GM, Rodriguez E, Nabiee R, Totonchy J, Mulama DH, Nyagol J, Wussow F, Barasa AK, Brehm M, Ogembo JG. 2019. Kaposi sarcoma-sssociated herpesvirus glycoprotein H is indispensable for infection of epithelial, endothelial, and fibroblast cell types. J Virol 93:e00630-19. https://doi.org/10.1128/JVI.00630-19.
32. Petherbridge L, Xu H, Zhao Y, Smith LP, Simpson J, Baigent S, Nair V. 2009. Cloning of Gallid herpesvirus 3 (Marek's disease virus serotype-2) genome as infectious bacterial artificial chromosomes for analysis of viral gene functions. J Virol Methods 158:11–17. https://doi.org/10.1016/j.jviromet.2009.01.009.
33. Rudd JS, Musarrat F, Kousoulas KG. 2021. Development of a reliable bovine neuronal cell culture system and labeled recombinant bovine herpesvirus type-1 for studying virus-host cell interactions. Virus Res 293: 198255. https://doi.org/10.1016/j.virusres.2020.198255.
34. Silva RF, Dunn JR, Cheng HH, Niikura M. 2010. A MEQ-deleted Marek's disease virus cloned as a bacterial artificial chromosome is a highly efficacious vaccine. Avian Dis 54:862–869. https://doi.org/10.1637/9048-090409-Reg.1.
35. Kamel M, El-Sayed A. 2019. Utilization of herpesviridae as recombinant viral vectors in vaccine development against animal pathogens. Virus Res 270:197648. https://doi.org/10.1016/j.virusres.2019.197648.
36. Suter M, Hefti HP. 2004. Protective DNA vaccination by particle bombardment using BAC DNA containing a replication-competent, packaging-defective genome of herpes simplex virus type I. Methods Mol Biol 256: 303–308. https://doi.org/10.1385/1-59259-753-X:303.
37. Tang N, Zhang Y, Pedrera M, Chang P, Baigent S, Moffat K, Shen Z, Nair V, Yao Y. 2018. A simple and rapid approach to develop recombinant avian herpesvirus vectored vaccines using CRISPR/Cas9 system. Vaccine 36: 716–722. https://doi.org/10.1016/j.vaccine.2017.12.025.
38. Tang N, Zhang Y, Shen Z, Yao Y, Nair V. 2021. Application of CRISPR-Cas9 Editing for Virus Engineering and the Development of Recombinant Viral Vaccines. Crispr j 4:477–490. https://doi.org/10.1089/crispr.2021.0017.
39. Teng M, Yao Y, Nair V, Luo J. 2021. Latest advances of virology research using CRISPR/Cas9-based gene-editing technology and its application to vaccine development. Viruses 13:779. https://doi.org/10.3390/v13050779.
40. Posfai G, Plunkett G, 3rd, Feher T, Frisch D, Keil GM, Umenhoffer K, Kolisnychenko V, Stahl B, Sharma SS, de Arruda M, Burland V, Harcum SW, Blattner FR. 2006. Emergent properties of reduced-genome *Escherichia coli*. Science 312:1044–1046. https://doi.org/10.1126/science.1126439.
41. Heming JD, Conway JF, Homa FL. 2017. Herpesvirus capsid assembly and DNA packaging. Adv Anat Embryol Cell Biol 223:119–142. https://doi.org/10.1007/978-3-319-53168-7_6.
42. Kumar PK, Maschke HE, Friehs K, Schügerl K. 1991. Strategies for improving plasmid stability in genetically modified bacteria in bioreactors. Trends Biotechnol 9:279–284. https://doi.org/10.1016/0167-7799(91)90090-5.
43. Claus-Henning N, Pohlmann A, Sodeik B. 2014. Construction and characterization of bacterial artificial chromosomes (BACs) containing herpes simplex virus full-length genomes, p 43–62. *In* Diefenbach RJ, Fraefel C (ed), Herpes simplex virus methods and protocols. Humana Press, New York, NY.
44. Cunningham C, Davison AJ. 1993. A cosmid-based system for constructing mutants of herpes simplex virus type 1. Virology 197:116–124. https://doi.org/10.1006/viro.1993.1572.
45. Leem SH, Yoon YH, Kim SI, Larionov V. 2008. Purification of circular YACs from yeast cells for DNA sequencing. Genome 51:155–158. https://doi.org/10.1139/g07-109.
46. Noskov VN, Chuang RY, Gibson DG, Leem SH, Larionov V, Kouprina N. 2011. Isolation of circular yeast artificial chromosomes for synthetic biology and functional genomics studies. Nat Protoc 6:89–96. https://doi.org/10.1038/nprot.2010.174.
47. Martin DW, Deb SP, Klauer JS, Deb S. 1991. Analysis of the herpes simplex virus type 1 OriS sequence: mapping of functional domains. J Virol 65: 4359–4369. https://doi.org/10.1128/JVI.65.8.4359-4369.1991.
48. Tripathy DN, Garcia M. 2008. Laryngotracheitis, p 94–98. *In* Swayne DE, Glisson JR, Jackwood MW, Pearson JE, Reed WM (ed), Isolation and identification of avian pathogens, 5th edition. University of Pennsylvania, New Bolton Center, PA.
49. Arad U. 1998. Modified hirt procedure for rapid purification of extrachromsomal DNA form mammalian cells. Biotechniques 24:760–762. https://doi.org/10.2144/98245bm14.
50. Pater MM, Hyman RW, Rapp F. 1976. Isolation of herpes simplex virus DNA from the "hirt supernatant". Virology 75:481–483. https://doi.org/10.1016/0042-6822(76)90046-5.
51. Fuchs W, Mettenleiter TC. 1996. DNA sequence and transcriptional analysis of the UL1 to UL5 gene cluster of infectious laryngotracheitis virus. J Gen Virol 77:2221–2229. https://doi.org/10.1099/0022-1317-77-9-2221.
52. Dretzen G, Bellard M, Sassone-Corsi P, Chambon P. 1981. A reliable method for the recovery of DNA fragments from agarose and acrylamide gels. Anal Biochem 112:295–298. https://doi.org/10.1016/0003-2697(81)90296-7.
53. Garcia M, Spatz SJ, Cheng Y, Riblet SM, Volkening JD, Schneiders GH. 2016. Attenuation and protection efficacy of ORF C gene-deleted recombinant of infectious laryngotracheitis virus. J Gen Virol 97:2352–2362. https://doi.org/10.1099/jgv.0.000521.
54. Korz DJ, Rinas U, Hellmuth K, Sanders EA, Deckwer WD. 1995. Simple fed-batch technique for high cell density cultivation of *Escherichia coli*. J Biotechnol 39:59–65. https://doi.org/10.1016/0168-1656(94)00143-z.
55. Di Tommaso P, Chatzou M, Floden EW, Barja PP, Palumbo E, Notredame C. 2017. Nextflow enables reproducible computational workflows. Nat Biotechnol 35:316–319. https://doi.org/10.1038/nbt.3820.
56. Andrews S. 2010. "FastQC: a quality control tool for high throughput sequence data." http://www.bioinformatics.babraham.ac.uk/projects/fastqc/. Accessed
57. Kruege F. 2019. A wrapper tool around Cutadapt and FastQC to consistently apply quality and adapter trimming to FastQ files, with some extra functionality for MspI-digested RRBS-type (Reduced Representation Bisufite-Seq) libraries. http://www.bioinformatics.babraham.ac.uk/projects/trim_galore/. Accessed
58. Anonymous. 2019. BBDuk: filters, trims, or masks reads with kmer matches to an artifact/contaminant file. https://sourceforge.net/projects/bbmap/. Accessed
59. Chevreux B, Wetter T, Suhai S. 1999. Genome Sequence Assembly using Trace Signal and Additional Sequence information. Computer Science and Biology GCB 1:45–56.
60. Sommer DD, Delcher AL, Salzberg SL, Pop M. 2007. Minimus: a fast, lightweight genome assembler. BMC Bioinformatics 8:64. https://doi.org/10.1186/1471-2105-8-64.
61. Staden R, Judge D, Bonfield JK. 2003. Managing sequencing projects in the GAP4 environment. *In* Krawetz SA, Wombie DD (ed), Introduction to bioinformatics: a theoretical and practical approach Humana Press Inc, Titowas, NJ.
62. Rodríguez-Avila A, Oldoni I, Riblet S, García M. 2007. Replication and transmission of live-attenuated infectious laryngotracheitis virus (ILTV) vaccines. Avian Dis 51:905–911. https://doi.org/10.1637/8011-041907-REGR.1.
63. Devlin JM, Browning GF, Hartley CA, Kirkpatrick NC, Mahmoudian A, Noormohammadi AH, Gilkerson JR. 2006. Glycoprotein G is a virulence factor in infectious laryngotracheitis virus. J Gen Virol 87:2839–2847. https://doi.org/10.1099/vir.0.82194-0.
64. Lee SW, Hartley CA, Coppo MJ, Vaz PK, Legione AR, Quinteros JA, Noormohammadi AH, Markham PF, Browning GF, Devlin JM. 2015. Growth kinetics and transmission potential of existing and emerging field strains of infectious laryngotracheitis virus. PLoS One 10:e0120282. https://doi.org/10.1371/journal.pone.0120282.
65. Vagnozzi A, Zavala G, Riblet SM, Mundt A, Garcia M. 2012. Protection induced by commercially available live-attenuated and recombinant viral vector vaccines against infectious laryngotracheitis virus in broiler chickens. Avian Pathol 41:21–31. https://doi.org/10.1080/03079457.2011.631983.
66. Johnson DI, Vagnozzi A, Dorea F, Riblet SM, Mundt A, Zavala G, Garcia M. 2010. Protection against infectious laryngotracheitis by in ovo vaccination with commercially available viral vector recombinant vaccines. Avian Dis 54:1251–1259. https://doi.org/10.1637/9401-052310-Reg.1.
67. Vagnozzi A, Riblet SM, Zavala G, Garcia M. 2012. Optimization of a duplex real-time PCR method for relative quantitation of infectious laryngotracheitis virus. Avian Dis 56:406–410. https://doi.org/10.1637/9883-081111-ResNote.1.
68. Zhao W, Spatz S, Zhang Z, Wen G, Garcia M, Zsak L, Yu Q. 2014. Newcastle disease virus (NDV) recombinants expressing infectious laryngotracheitis virus (ILTV) glycoproteins gB and gD protect chickens against ILTV and NDV challenges. J Virol 88:8397–8406. https://doi.org/10.1128/JVI.01321-14.
69. Livak KJ, Schmittgen TD. 2001. Analysis of relative gene expression data using real-time quantitative PCR and the 2(-Delta Delta C(T)). Method Methods 25:402–408. https://doi.org/10.1006/meth.2001.1262.